

A Multidrug Delivery System Using a Piezoelectrically Actuated Silicon Valve Manifold With Embedded Sensors

Allan T. Evans, Srinivas Chiravuri, and Yogesh B. Gianchandani, *Fellow, IEEE*

Abstract—This paper describes a drug delivery system for chronic pain that can accommodate multidrug protocols. An element that is important to the function of the system is a customized silicon micromachined valve manifold. Each valve is piezoelectrically actuated and operates by pressing an elongated valve seat against a shared glass substrate. The dual-valve substrate has two inlets and one outlet; a piezoresistive pressure sensor is embedded in the Si structure near each of these three ports. The sensors, which permit closed-loop control and error monitoring of the flow rate, have a typical sensitivity of 698 ppm/kPa. The $1 \times 1.5 \times 3 \text{ cm}^3$ manifold provides modulation and mixing capabilities. The manifold is integrated into a stainless steel housing with a total volume of 130 cm^3 and a reservoir volume of 40 cm^3 . Two spring-loaded polyethylene reservoirs feed the valve manifold at pressures up to 0.52 kPa/mL. Benchtop tests of bolus and continuous flow delivery demonstrate flow rates ranging from 2.30 to 0.51 mL/h. (Both larger and smaller rates can be achieved by adjusting the parameters of the manifold valves or reservoir springs.) Additional tests suggest that the system can compensate for changes in spinal fluid pressure and that pressure profiles can be used to detect catheter occlusions and disconnects. [2010-0186]

Index Terms—Drug delivery, liquid flow, manifold, microvalve, piezoelectric.

I. INTRODUCTION

CHRONIC PAIN impacts over 100 million Americans with annual treatment costs exceeding \$100 billion [1], [2]. One treatment for severe chronic pain is the implantation of an intrathecal drug delivery device (IDDD) [3]–[7]. Conventionally, an IDDD that allows active control of the delivery rate is composed of several components other than the drug reservoir, including a peristaltic pump, a control circuit, and a battery. The inclusion of these components reduces the fractional volume of the unit that may be occupied by the drug itself; this is considered the volume efficiency ratio (VER). An alternative architecture that uses throttle valves to regulate flow from pressurized drug reservoirs can potentially improve the VER

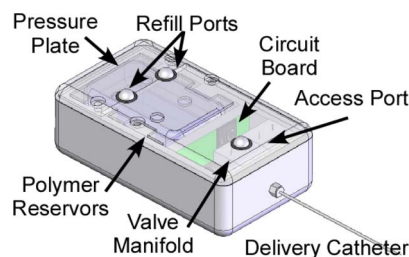


Fig. 1. System overview: Two polymer reservoirs are pressed by a plate attached to compressive springs to generate pressure. Two valves in a manifold are used to regulate drug delivery rates. Control is regulated by onboard electronics that allow for pressure monitoring and reprogramming.

by obviating the pump [8]. This architecture is also appealing for multidrug delivery systems.

Delivery of multiple drugs into the intrathecal space is utilized in clinical practice when monodrug therapy with opioids fails, either due to tolerance, opioid nonresponsiveness (neuropathic pain), or hyperalgesia [9], [10]. Current practice consists of mixing multiple drugs in a single chamber for simultaneous delivery into spinal fluid [11]–[13]. This constrains the type and concentration of drugs that can be administered.

In this paper, we explore an IDDD system architecture that utilizes a silicon micromachined two-valve manifold to regulate flow from pressurized reservoirs (Fig. 1). Piezoelectric actuation is used for power efficiency. The manifold also includes three pressure sensors that may be used to determine delivery rates.¹ A system with multiple independently regulated drug reservoirs can improve analgesic efficacy, reduce treatment cost, and ultimately improve patient satisfaction. This method of combination therapy also limits side effects because it uses the lowest possible doses of each drug. The design, fabrication, and testing of the valve manifold are discussed in Section II. The system assembly and test results are presented in Section III. Section IV contains the discussion and a summary overview.

II. MANIFOLD DESIGN AND TESTING

The valve manifold should modulate liquid flow from less than 0.5 mL/day to more than 5 mL/day from each reservoir independently, although typical delivery rates average near the middle of that range. Both the valve and the embedded pressure sensors should be able to accommodate pressures as high as

Manuscript received June 20, 2010; revised August 29, 2010; accepted October 20, 2010. Date of publication December 23, 2010; date of current version February 2, 2011. Subject Editor S. Shoji.

A. T. Evans and Y. B. Gianchandani are with the Department of Electrical Engineering and Computer Science, University of Michigan, Ann Arbor, MI 48109-2122 USA (e-mail: evansall@umich.edu; yogesh@umich.edu).

S. Chiravuri is with the Department of Anesthesiology, University of Michigan, Ann Arbor, MI 48109-5048 USA (e-mail: srinivas@umich.edu).

Color versions of one or more of the figures in this paper are available online at <http://ieeexplore.ieee.org>.

Digital Object Identifier 10.1109/JMEMS.2010.2093566

¹Portions of this paper appear in conference abstract form in [14].

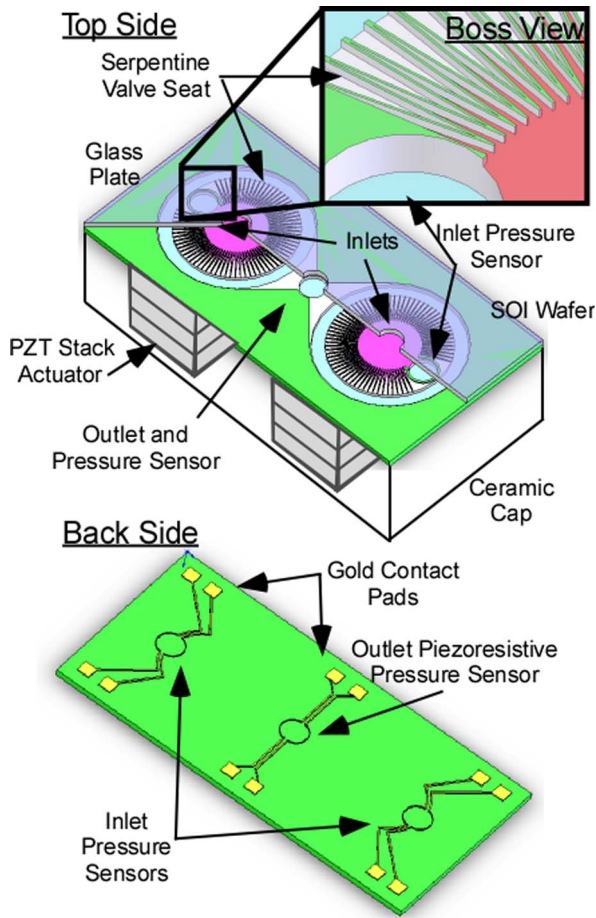


Fig. 2. On the top side of the Si wafer, which is the substrate side of an SOI wafer, there are two membranes with serpentine valve seats. Each one is located on a central boss that also houses a pressure sensor and presses against a glass plate that has two inlets and an outlet. The back side, which is the epitaxial side of the SOI wafer, has boron doping and gold traces for the pressure sensors.

100 kPa. (The precise load will depend on the targeted range of delivery pressure and the drug volume remaining in the reservoir.) While actuation mechanisms used in microsystems range from electrostatic to thermal phase change, this system favors piezoelectric actuation because this approach consumes low power and generates forces that allow valve operation across a wide range of operating pressures [15]–[24]. A silicon-on-insulator (SOI) wafer is used for the manifold to ease the fabrication of embedded sensors. The pressure sensors use implanted piezoresistors and target a sensitivity of at least 600 ppm/kPa for accurate feedback control.

The manifold (Fig. 2) operates by pressing elongated silicon valve seats against a glass wafer using piezoelectric actuators. The elongated valve seat increases the flow perimeter which compensates for the limited deflection of the piezoelectric actuators [25]. The piezoelectric actuators used in the manifold are commercially available lead zirconate titanate (PZT) stacks. The valves throttle by constricting the flow path from the reservoirs to the intrathecal space. The 0–2- μm spacing between the valve seat and the glass plate creates a channel that has a much higher hydraulic resistance than the delivery catheter. The small size and low power consumption of the manifold allow

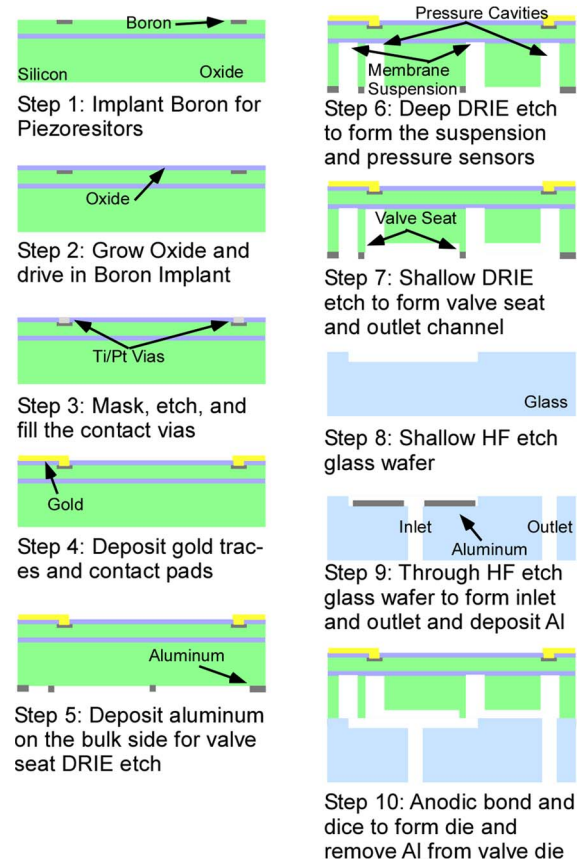


Fig. 3. Si–glass micromachining process: Sensors are formed on the device layer of the SOI wafer by implanting boron and making ohmic connections through a field oxide to gold contact pads on the device perimeter. The buried oxide layer in the SOI wafer acts as an etch stop for DRIE when forming membranes. A two-step DRIE process is illustrated for the SOI wafer. A glass wafer undergoes two wet etch steps for a recess and through-hole formation. Next, the two wafers are bonded and diced.

for larger reservoirs and smaller batteries to be used without increasing the size of an implantable system.

A. Fabrication

The manifold is fabricated from an SOI wafer with layer thicknesses of 20, 2, and 450 μm and a 500- μm -thick Pyrex glass wafer. The SOI and glass wafers are independently processed and bonded prior to singulation. The fabrication processes for the SOI and glass wafers are shown in Fig. 3.

For the SOI wafers, the first step is to form the piezoresistors for the pressure sensors on the device side of the wafers. Boron implantation is performed with a $1 \times 10^{13} \text{ cm}^{-2}$ dose at an energy level of 20 keV with a 7° tilt. The implantation, drive-in, and annealing temperatures were calculated using the TSUPREM-4 implantation simulator and selected to yield a carrier profile that provides at least 600-ppm/kPa sensitivity. The simulations indicate that the resistors should have a sheet resistance of about $5.3 \times 10^3 \Omega/\square$ and a resistance of 112.6 k Ω .

After the boron implantation, a thermal oxidation step provides both the necessary isolation and the high-temperature anneal needed to activate and diffuse the implanted boron. A 1000- \AA -thick oxide is grown at 1000 $^\circ\text{C}$ for 20 min, and

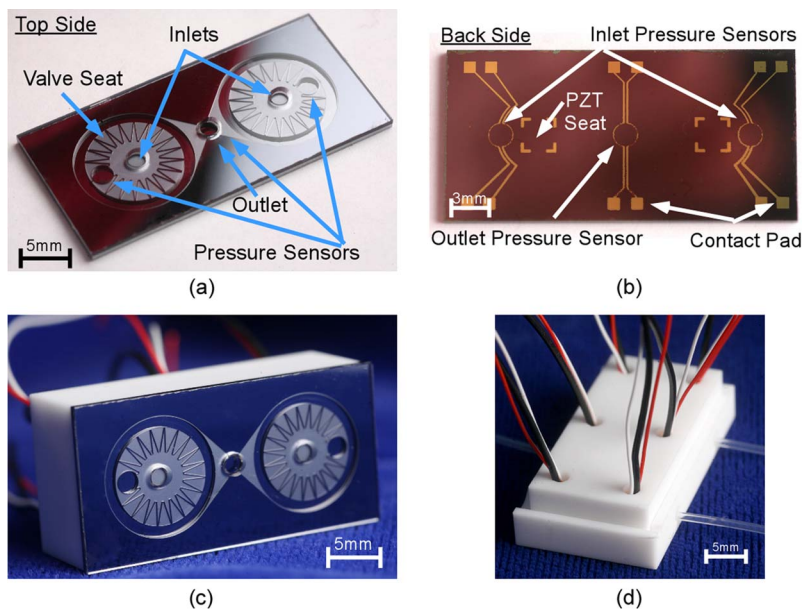


Fig. 4. Photographs of a fabricated valve manifold. (a) The glass inlets and outlets, the two valve seats, and the pressure sensor cavities are clearly visible on the top. (b) The gold contact pads and traces for the pressure sensors and the gold to define the PZT locations are clearly visible on the back side of the device. (c) Both valve plates are clearly visible, and the common outlet port is located in the center of the die. The manifold measures $3 \times 1.5 \times 1.1 \text{ cm}^3$. (d) Inlets and outlet tubes of the assembled header interface with the valve through a Macor connector piece.

the wafer is left in a nitrogen environment for an additional 5 min to allow enough diffusion time for the implanted boron. Vias are etched in the oxide using buffered hydrofluoric acid (BHF) to create contacts to the buried piezoresistors, and metal is deposited on the wafer to make ohmic contact with the boron-doped silicon. A platinum/gold (500/1000-Å-thick) layer with a titanium adhesion layer (50 Å) is evaporated onto the wafer and put in acetone to pattern via lift off. Lastly, more gold (1000 Å) is evaporated with a chrome adhesion layer (300 Å) to form the conductive traces and contact pads for easier electrical interface with external wiring. Fig. 4 shows the fabricated manifold with a standard starburst pattern.

After the device side is processed, the back side of the wafer is subjected to two deep reactive-ion etch (DRIE) process steps to create the pressure sensor diaphragms, the valve membrane suspension, and the serpentine grooves that provide the elongated flow perimeter. The two-step DRIE process uses aluminum and photoresist masks to achieve the desired groove and membrane structures. The resulting grooves are 120 μm in depth and provide a seat perimeter that is 81 mm long. (Other versions of this valve had perimeter lengths of 315 and 14 mm; under similar operating conditions, these would be appropriate for higher and lower flow rates, respectively.)

A Pyrex glass wafer is patterned with a 1.4- μm recess using BHF and is then subjected to a HF etch to form through vias that act as the valve inlets and outlets. After the recess is formed, both sides of the glass wafer are patterned with chrome, gold, and a thick photoresist. The wafer is then placed in HF until the through holes are etched. After stripping the etch mask, a thin film layer of sacrificial aluminum is deposited through evaporation into the recessed areas to prevent inadvertent bonding in the next step. The SOI and glass wafers are then anodically bonded at 400 °C, and the wafers are diced to create the final valve die.

After the valves are fabricated, solder connections are made to the pressure sensor pads, and they are assembled with the PZT actuator stack inside a ceramic Macor cap. The valve plates on the manifold can be individually adjusted during the bond step to create a normally open, a partially open, or a normally closed valve. More information on this method of assembly is provided in [26]. The final manifold structure measures $3 \times 1.5 \times 1.1 \text{ cm}^3$ when assembled with a Macor header to provide fluid interconnects. The assembled structure is shown in Fig. 4.

B. Experimental Results

Partially open manifold valves were tested for gas and liquid regulation at room temperature. Gas flow experimentation was conducted using pressurized nitrogen and is presented in [27]. For liquid modulation testing, experiments were conducted using regulated nitrogen gas to pressurize a liquid reservoir. Pressure-driven isopropyl alcohol (IPA) flow was regulated into the individual inlets of the manifold by external valves [Fig. 5(a)]. Flow leaving the valve manifold (or single valve) was determined by recording the travel of air bubbles along a 1-m-long catheter at the outlet of the device. The catheter is similar in length and size to those used in intrathecal drug delivery implants. This mimics the output resistance experienced in the drug delivery system and allows for more accurate characterization of the liquid flow rate as it pertains to the targeted system application.

C. Liquid Flow Tests

Liquid modulation tests were conducted on the manifolds to determine flow properties and mixing from the independently regulated reservoirs. In a typical test, flow from valve A (one

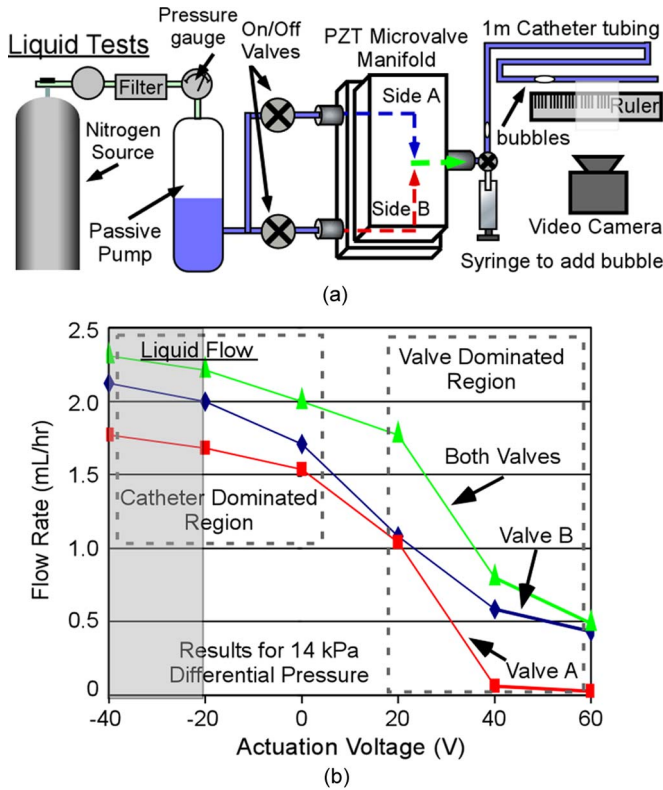


Fig. 5. (a) Valve test setup. Nitrogen is used to pressure fluid in a large reservoir. The pressurized fluid is independently routed to each side of the manifold, and a video camera records the travel of bubbles through a 1-m catheter tube to determine the flow rate through the valve. (b) Flow rate of alcohol through individual and combined valves in a manifold at 14 kPa. The catheter resistance is greater than the valve resistance at low voltages outside the preferred operating region. This results in reduced modulation. Mixing also functions as expected and is particularly evident in the lower flow rate regimes.

side of the manifold) varied from 1.77 to 0.028 mL/h, and flow from valve B varied from 2.12 to 0.38 mL/h in an 80-V actuation range [Fig. 5(b)]. When both valves A and B were open together, the flow rates were combined from each valve within two separate flow regimes. At high flow rates, the catheter resistance dominated the flow. At lower flow rates, the valve resistance dominated, and the combined flow rates were close to the individual flow rates of each valve added together.

Several piezoresistors were tested at room temperature, and the resistance varied between 100 and 150 k Ω , indicating close correspondence with the simulation. The pressure sensors were driven at 5 V as the differential output voltage was monitored. Multiple pressure sensors were monitored over 3 d to determine linearity and sensitivity. At room temperature, the pressure sensors showed a sensitivity of 698 ppm/kPa, which exceeds our minimum target for this application.

III. SYSTEM RESULTS

This section describes the system assembly, flow tests, and safety experiments. A prototype of a drug delivery system is shown in Fig. 6. The system was operated using a custom-designed control printed circuit board that operated from a 3.3-V battery. Flow control from multiple reservoirs was tested using both continuous regulation and duty-cycle regulation.

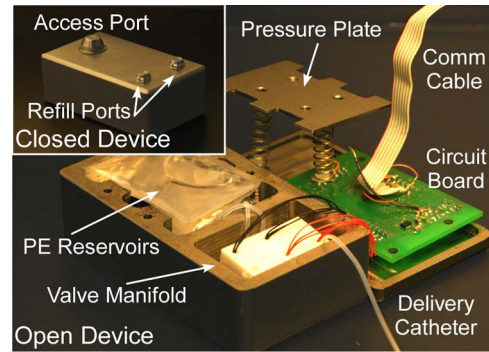


Fig. 6. Drug delivery prototype pictured during assembly. Two polymer reservoirs are pressurized using a spring-loaded plate. Flow is monitored and regulated by a PZT-actuated valve manifold with embedded pressure sensors. The entire system takes up about 130 cm³. The inset shows a photograph of the closed system with the refill and catheter access ports.

Failure mode testing indicates that embedded pressure sensors can be used to detect certain failures that are possible during deployment.

A. Housing, Assembly, and Components

The system requires development of a biologically compatible housing with integrated components that are necessary for delivery monitoring and regulation. This prototype is made from stainless steel using traditional machining. An actual realization of the IDDD would likely be made of biocompatible titanium. The stainless steel housing contains a two-valve manifold, a control circuitry, two polyethylene (PE) reservoirs, a steel pressure plate, traditional springs, and a battery. The system housing measures 5.08 cm \times 9 cm \times 3 cm, with 5-mm beveled edges. The housing has a total volume of 130 cm³ with a total reservoir volume of 40 cm³. This prototype has a VER of 30.7%, but it can be increased by integrating the system components into the housing more efficiently.

The drug delivery system has three ports. Two of these are standard refill ports (Instech Laboratories, Plymouth Meeting, PA; model MIC) that are connected to the two reservoirs by tubing. The ports have a silicone elastomer septum, an open cavity, and a metal base plate and are integrated into the system casing. These ports permit the reservoirs to be filled by a syringe equipped with a Huber needle. The third port is a fluidic access port. The port is connected directly to the catheter to allow a physician to circumvent the device for direct access to the cerebrospinal fluid.

The PE reservoirs in this prototype are pressurized through compression by a metal plate [Fig. 7(a)]. The reservoirs have an inlet tube from the refill port and exit tubing to the manifold and its inlet pressure sensors. The reservoirs are fabricated by heat-sealing PE into the desired shape to fit within the housing cavity designed for the pressure plate. The reservoirs are stacked; compressed springs drive the pressure plate against the top reservoir, which, in turn, presses against the bottom reservoir. There are vertical guides in the plate and in the casing to maintain alignment of the plate, springs, and reservoirs during the assembly and compression. The pressure response of the reservoir can be adapted to specific system needs by

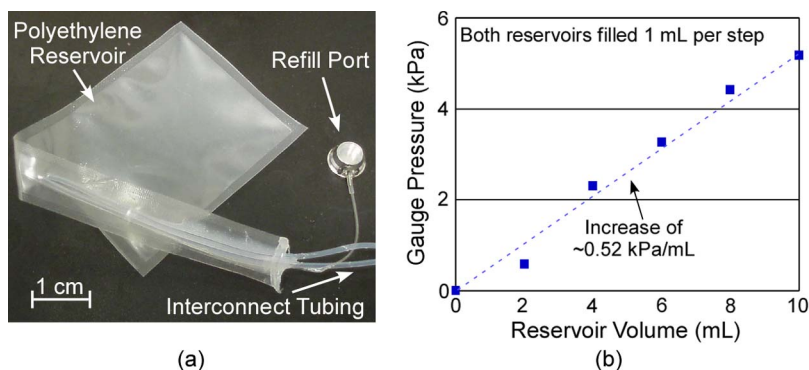


Fig. 7. (a) Photograph of a reservoir before it is inserted into the system. The reservoir is connected to the refill port and interconnect tubing that leads to the manifold and a pressure sensor. (b) Results from one reservoir filling test where each reservoir was filled with IPA in 1-mL increments. The results for fill volumes up to 10 mL suggest a linear pressure profile of 0.52 kPa/mL.

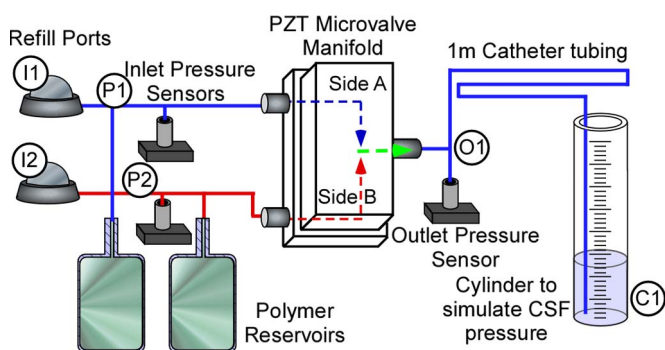


Fig. 8. Schematic of the entire system under test. A cylinder at the outlet of the device is used to simulate intrathecal pressure. The schematic is labeled to signify important nodes at which partial system test results may be monitored.

appropriately selecting the compressive springs used to drive the pressure plate. In this case, two centralized compressive springs pressurized the reservoirs. The springs were characterized by filling the reservoirs with a control volume of liquid (1 mL, IPA) and measuring the resultant pressure using the internal pressure sensors. (For this test, the reservoir outlets were sealed to prevent outflow.) The pressures varied from 0 kPa when completely empty to 5.17 kPa at 10 mL of total volume [Fig. 7(b)]. This represents a typical increase of 0.52 kPa/mL which is acceptable for system functionality.

B. Experimental Methods

The experimental evaluation method allowed the entire flow path to be tested from the refill ports, through the system, to a delivery catheter with a pressure load that mimicked intrathecal load pressure (Fig. 8). The method also permitted testing of the sensors to detect certain system-level faults that could occur during deployment. Three variants of the test structure were used. Tests of the complete system used absolute pressure sensors at the inlet and outlet ports (Freescale MPXA4250 at each inlet; Freescale MPXA6115 at the outlet) in addition to the readings available from the manifold pressure sensors. A second variant replaced the dual polymer reservoirs with a single inlet that delivered liquid under steady pressure from a nitrogen canister using feedback and set-point control. In this scheme, only one side of the manifold was used for testing.

The second valve in the manifold was flooded with IPA (to remove all air bubbles from the device) and was sealed at the inlet to allow no air in or alcohol out. The inlet pressure sensor was a Baratron absolute pressure sensor from MKS. The third variant used the complete system schematic, except that, instead of using two pressurized reservoirs, one channel was sealed and only one reservoir was used. This variant was used to test individual channels via superposition before testing the finished system.

C. System-Level Delivery Tests

Typically, the intrathecal pressure for cerebrospinal fluid varies from 0.7 to 1.8 kPa in healthy adults [28]. This pressure load was mimicked in the experimental procedure by locating the outlet of the delivery catheter at the bottom of a column of water. The level in the column was varied to reflect the ranges of pressure differences that can occur in the human body. Detection of, and compensation for, this pressure variation can be achieved by using the outlet pressure sensor of the manifold.

Experimental characterization of the manifold outlet pressure sensor at a fixed valve aperture provided a linear relationship between the sensor output and the load pressure of 35.8 mV/kPa. Further details are available in [27].

This information was used, together with the data from flow characterization of the manifold, to create a microcontroller program that compensated the aperture to maintain a set flow rate against variation in load pressure. Fig. 9 compares experimentally the observed flow rates that compensate for variations in delivery pressure to the uncompensated flow rates. (These data were acquired using the second variant of the test setup.) The uncompensated flow rates decreased from 0.58 down to 0.21 mL/h as the load pressure was increased by 1.5 kPa. In contrast, the compensated flow program adjusted the manifold to maintain a flow rate of 0.58 mL/h while remaining within 0.5% across the range.

In controlled flow tests, both reservoirs, pressurized by the springs, were filled via the refill ports and used for delivery through the manifold. The flow rate through the manifold was modulated by varying the duty cycle of a 0–60-V square wave running at 0.02 Hz. In a typical test (Fig. 10), three target flow rates were programmed over a 200-min period, and the resultant

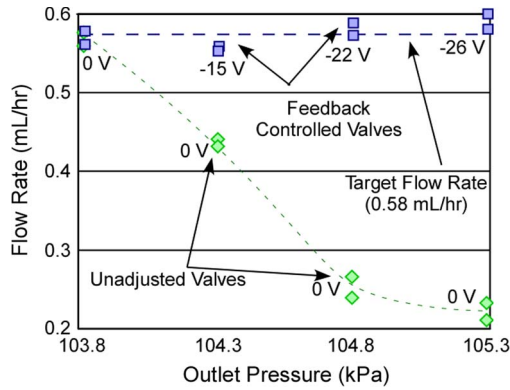


Fig. 9. Flow and actuation voltages for changing heights of cylinder pressures to represent unregulated and regulated flows using the internal pressure sensor. Unregulated flow varied from 0.58 to 0.21 mL/h, while regulated flow remained within 0.5% of the target flow rate. The results suggest that the outlet pressure sensor can be used to compensate to maintain delivery across intrathecal pressure variation.

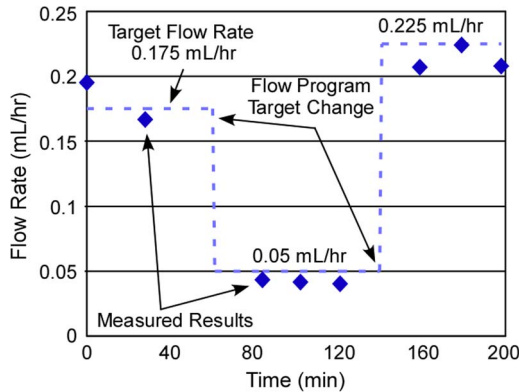


Fig. 10. Typical duty-cycle regulation of flow through the manifold with multiple set points. In this instance, the duty cycle of a 60-V square wave at 0.02 Hz is altered to achieve mixed flow at the target delivery rates. Controllable delivery from multiple reservoirs was achieved with performance acceptable for clinical applications.

output was measured. (These data were acquired using the third variant of the test setup.) The instantaneous deviation from the set flow rate was no more than 0.01 mL/h. All flow rates were well within medical limits, with less than 15% deviation from the target delivery rate [29]. The average supply voltage to the system was 3.3025 V, and the average current draw was 18 mA. Neglecting the power draw from the electronics, this suggests a typical unoptimized power draw of 57.6 mWh for the system during operation.

D. Failure Mode Testing

As noted previously, the inclusion of pressure sensors with the drug delivery device permits the detection of failure modes such as catheter kinks (or tip occlusions) and catheter disconnects from the pump or displacement from the intrathecal space [30]. Traditionally, changes in the disposition of the catheter are detected by symptoms related to the consequent alterations in medication rates. Basically, if the patient receives no analgesic benefit despite a change in dose, an occluded or disconnected

catheter should be suspected and investigated to prevent acute medication withdrawal which can be life threatening in the case of baclofen. The physician may then use one of several techniques to determine the actual alterations in the catheters, from tracing radioactive dye through the delivery chain to surgical investigation. By appropriately utilizing the pressure sensors, the system can potentially detect these conditions before the patient experiences discomfort or withdrawal.

The pressure response for catheter kinks was tested by flowing IPA at a constant rate through the manifold and out the catheter into an air ambient environment. In an effort to simulate the effects of a kink or occlusion, the tip of the catheter was completely occluded, and the response was measured on an oscilloscope. The duration of the occlusion was varied to determine the sensor response to temporary blocks or severe kinks [Fig. 11(a)]. (These data were acquired using the first variant of the test setup.) The outlet pressure was 100.3 kPa, while IPA was flowing from an unoccluded catheter. Occlusion of the catheter provided an average pressure ramp of 90 Pa/s while the catheter remained blocked. This pressure ramp was repeatable and steeper than any encountered during normal operation.

The pressure response of the disconnection of the catheter from the pump was tested in a manner that is similar to the tests for catheter occlusions. The transient pressure at the outlet of the pump was recorded prior to the manual separation of the catheter from the pump, while the catheter remained disconnected, and after reattachment of the catheter [Fig. 11(b)]. The tests indicate a significant initial drop in the pump outlet pressure at the time of the disconnect. The pressure then settles at a new value. Although the *in vivo* pressure change is likely to be lower in magnitude than the typical response in an air ambient, it appears likely that a rapid drop in the outlet pressure will signify acute disconnects.

E. Magnetic Field Compatibility

Magnetic resonance imaging (MRI) is a relatively common medical diagnostic technique in which the patient is exposed to very strong magnetic fields. The long-term implantation of an IDDD makes it likely that some patients with implants will require MRI. Drug pumps that are driven by electromagnetic motors typically cease operation during an MRI procedure. The absence of a magnetic motor in this work suggests that it may be naturally more accommodating of MRI conditions. As noted previously, even in the powered-off condition, the valves can be designed to provide a moderate level of drug delivery, should this be necessary.

Preliminary magnetic compatibility tests for the system were conducted on the manifold to determine changes that occur due to the presence and orientation of a magnetic field. A magnetic field of 453 G was generated across the manifold with varying orientation. While this field is significantly weaker than the strongest fields generated by MRI machines, the preliminary indication from this test is consistent with expectations. Tests used IPA flowing through one inlet while blocking the second inlet. The flow was measured with no magnetic field and with the field oriented along the x -, y -, and z -axes of the manifold.

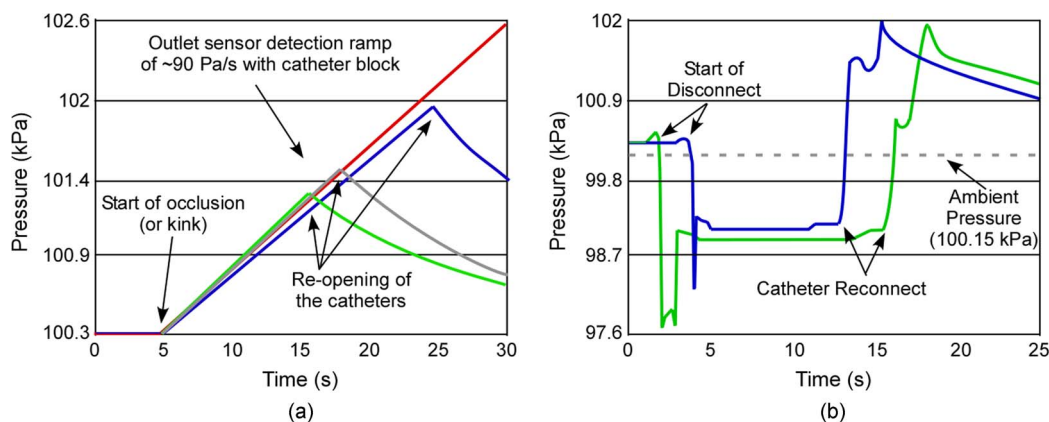


Fig. 11. (a) Outlet pressure before, during, and after the catheter is blocked. A pressure ramp of about 90 Pa/s is observed when the catheter is occluded. (b) Outlet pressure sensor when the catheter is disconnected and later reattached to the drug delivery device. The tests were conducted in air ambient; some aspects of the response may vary with test conditions.

For target flow rates of both 1 and 0.67 mL/h, there was no measurable variation. These initial tests suggest that PZT actuators in a valve manifold are not measurably affected by magnetic fields of this magnitude.

IV. CONCLUSION

This effort has resulted in the design and implementation of a prototype drug delivery system for use in testing aspects of multidrug protocols with a valve-regulated architecture. A piezoelectrically actuated valve manifold with embedded inlet and outlet sensors was designed, fabricated, and used to regulate flow. Other components of the system included a pressurized plate for compressing two drug reservoirs. The components were integrated into a stainless steel housing with a total volume of 130 cm³. Several delivery tests were conducted for both bolus and continuous flow delivery using two reservoirs. Additional results suggest possible detection of catheter occlusions and disconnects. Testing also indicated that a system based on this architecture can compensate for changes in spinal fluid pressure. Although the valve manifold does not demonstrate sensitivity to moderate magnetic fields, further tests are necessary to determine the impact of MRI-strength magnetic fields.

The absence of a mechanical pump in this architecture potentially permits a great deal of flexibility in the form factor. The syringe pressure in the reservoirs and the modulation range of the valve manifold can be similarly adapted to a variety of applications. In summary, valve-regulated drug delivery holds promise as a volume-efficient, versatile, and safe architecture for a multidrug protocol system.

REFERENCES

- [1] "New standards to assess and manage pain," Joint Comm. Perspectives. Joint Comm. Accreditation Healthcare Org., vol. 19, no. 5, p. 5, Sep./Oct. 1999.
- [2] C. J. Phillips, "Pain management: Health economics and quality of life considerations," *Drugs*, vol. 63, no. 2, pp. 47–50, 2003.
- [3] M. Winkelmueller and W. Winkelmueller, "Long-term effects of continuous intrathecal opioid treatment in chronic pain of nonmalignant etiology," *J. Neurosurg.*, vol. 85, no. 3, pp. 458–467, Sep. 1996.
- [4] D. P. Wermeling, "Ziconotide, an intrathecally administered N-type calcium channel antagonist for the treatment of chronic pain," *Pharmacotherapy*, vol. 25, no. 8, pp. 1084–1094, Aug. 2005.
- [5] S. A. Schug, D. Saunders, I. Kurowski, and M. J. Paech, "Neuraxial drug administration: A review of treatment options for anesthesia and analgesia," *CNS Drugs*, vol. 20, no. 11, pp. 917–933, 2006.
- [6] R. L. Rauck, D. Cherry, M. F. Boyer, P. Kosek, J. Dunn, and K. Alo, "Long-term intrathecal opioid therapy with a patient-activated, implanted delivery system for the treatment of refractory cancer pain," *J. Pain*, vol. 4, no. 8, pp. 441–447, Oct. 2003.
- [7] T. Deer, I. Chapple, A. Classen, K. Javery, V. Stoker, L. Tonder, and K. Burchiel, "Intrathecal drug delivery for treatment of chronic low back pain: Report from the national outcomes registry for low back pain," *Pain Med.*, vol. 5, no. 1, pp. 6–13, Mar. 2004.
- [8] A. T. Evans, S. Chiravuri, and Y. B. Gianchandani, "A low power, microvalve regulated architecture for drug delivery systems," *Biomed. Microdevices*, vol. 12, no. 1, pp. 159–168, Feb. 2010.
- [9] S. J. Hassenbusch, R. K. Portenoy, M. Cousins, E. Buchser, T. R. Deer, S. L. D. Pen, J. Eisenach, K. A. Follett, K. R. Hildebrand, E. S. Krames, R. M. Levy, P. P. Palmer, J. P. Rathmell, R. L. Rauck, P. S. Staats, L. Stearns, and K. D. Willis, "Polyanalgesic consensus conference 2003: An update on the management of pain by intraspinal drug delivery—Report of an expert panel," *J. Pain Symptom Manage.*, vol. 27, no. 6, pp. 540–563, Jun. 2004.
- [10] E. S. Krames, "Practical issues when using neuraxial infusion," *Oncology (Williston Park)*, vol. 13, no. 5 Supplement 2, pp. 37–44, May 1999.
- [11] N. G. Rainov and V. Heidecke, "Management of chronic back and leg pain by intrathecal drug delivery," *Acta Neurochir. Suppl.*, vol. 97, pt. 1, pp. 49–56, 2007.
- [12] T. S. Grabow, D. Derdzinski, and P. S. Staats, "Spinal drug delivery," *Current Pain Headache Rep.*, vol. 5, no. 6, pp. 510–516, Dec. 2001.
- [13] V. C. Anderson and K. J. Burchiel, "A prospective study of long-term intrathecal morphine in the management of chronic nonmalignant pain," *Neurosurgery*, vol. 44, no. 2, pp. 289–301, 1999.
- [14] A. T. Evans, S. Chiravuri, and Y. B. Gianchandani, "A piezoelectric valve manifold with embedded sensors for multi-drug delivery protocols," in *Proc. Conf. MEMS*, 2010, pp. 1027–1030.
- [15] Y. Shinozawa, T. Abe, and T. Kondo, "A proportional microvalve using a bi-stable magnetic actuator," in *Proc. IEEE 10th Annu. Int. Workshop Micro Electro Mech. Syst.—An Investigation of Micro Structures, Sensors, Actuators, Machines and Robots*, 1997, pp. 233–237.
- [16] C. Fu, Z. Rummmler, and W. Schomburg, "Magnetically driven micro ball valves fabricated by multilayer adhesive film bonding," *J. Micromech. Microeng.*, vol. 13, no. 4, pp. S96–S102, Jul. 2003.
- [17] P. Dubois, B. Guldimmann, M. A. Gretillat, and N. F. de Rooij, "Electrostatically actuated gas microvalve based on a Ta–Si–N membrane," in *Proc. IEEE Int. Conf. MEMS*, 2001, pp. 535–538.
- [18] C. A. Rich and K. D. Wise, "A high-flow thermopneumatic microvalve with improved efficiency and integrated state sensing," *J. Microelectromech. Syst.*, vol. 12, no. 2, pp. 201–208, Apr. 2003.
- [19] S. Messner, M. Muller, V. Burger, J. Schaible, H. Sandmaier, and R. Zengerle, "A normally-closed, bimetallically actuated 3-way microvalve for pneumatic applications," in *Proc. 11th Annu. Int. Workshop*

Micro Electro Mech. Syst.—An Investigation of Micro Structures, Sensors, Actuators, Machines and Systems, 1998, pp. 40–44.

- [20] M. Kohl, D. Dittmann, E. Quandt, and B. Winzek, "Thin film shape memory microvalves with adjustable operation temperature," *Sens. Actuators A, Phys.*, vol. 83, no. 1–3, pp. 214–219, May 2000.
- [21] M. Esashi, S. Shoji, and A. Nakano, "Normally closed microvalve and micropump fabricated on a silicon wafer," *Sens. Actuators*, vol. 20, no. 1/2, pp. 163–169, Nov. 1989.
- [22] X. Yang, A. Holke, S. A. Jacobson, J. H. Lang, M. A. Schmidt, and S. D. Umans, "An electrostatic, on/off microvalve designed for gas fuel delivery for the MIT microengine," *J. Microelectromech. Syst.*, vol. 13, no. 4, pp. 660–668, Aug. 2004.
- [23] I. Chakraborty, W. C. Tang, D. P. Bame, and T. K. Tang, "MEMS microvalve for space application," *Sens. Actuators A, Phys.*, vol. 83, no. 1–3, pp. 188–193, May 2000.
- [24] D. C. Roberts, H. Li, J. L. Steyn, O. Yaglioglu, S. M. Spearing, M. A. Schmidt, and N. W. Hagood, "A piezoelectric microvalve for compact high-frequency, high-differential pressure hydraulic micropumping systems," *J. Microelectromech. Syst.*, vol. 12, no. 1, pp. 81–92, Feb. 2003.
- [25] T. R. Brosten, J. M. Park, A. T. Evans, K. Rasmussen, G. F. Nellis, S. A. Klein, J. R. Feller, L. Salerno, and Y. B. Gianchandani, "A numerical flow model and experimental results of a cryogenic micro-valve for distributed cooling applications," *Cryogenics*, vol. 47, no. 9/10, pp. 501–509, Sep./Oct. 2007.
- [26] J. M. Park, A. T. Evans, K. Rasmussen, T. R. Brosten, G. F. Nellis, S. A. Klein, and Y. B. Gianchandani, "A microvalve with integrated sensors and customizable normal state for low temperature operation," *J. Microelectromech. Syst.*, vol. 18, no. 4, pp. 868–877, Aug. 2009.
- [27] A. T. Evans, "Valve regulated implantable drug delivery for chronic pain management," Ph.D. dissertation, Univ. Michigan, Ann Arbor, MI, 2010.
- [28] B. Magnes, "Body position and cerebrospinal fluid pressure. Part I: Clinical studies on the effect of rapid postural changes," *J. Neurosurg.*, vol. 44, no. 6, pp. 687–697, Jun. 1976.
- [29] *Medtronic Synchronized II Programmable Pumps Implant Manual*, Medtronic, Fridley, MN, 2003.
- [30] S. Vaidyanathan, B. M. Soni, T. Oo, P. L. Hughes, G. Singh, J. W. H. Watt, and P. Sett, "Bladder stones—Red herring for resurgence of spasticity in a spinal cord injury patient with implantation of Medtronic Synchronized pump for intrathecal delivery of baclofen—A case report," *BMC Urology*, vol. 3, no. 3, 2003.
- [31] Medtronic, last accessed Jan. 2010 MRI Guidelines: The Effect of Magnetic Resonance Imaging (MRI) on Medtronic Infusion Systems. [Online]. Available: <http://professional.medtronic.com/devices/synchromed-el-for-spasticity/mri-guidelines/index.htm#synchromedII>



Allan T. Evans was born in Marquette, MI, in 1983. He received the B.S. degree in electrical engineering from Michigan State University, East Lansing, in 2005, and the M.S. degree in electrical engineering and the Ph.D. degree from the University of Michigan, Ann Arbor, in 2007 and 2010, respectively.

He is presently working internationally as a founder and director for Globe Shares Inc., a 501c3 charity based in Brighton, MI.



Srinivas Chiravuri received the M.D. degree from the University of Michigan, Ann Arbor, where he completed his Anesthesiology and Pain Medicine fellowship training.

He is presently an Assistant Professor of Anesthesiology/Pain Medicine at the University of Michigan, where he also serves as the Director for Neuromodulation and the Pain Medicine Fellowship. His research interests include all aspects of device-related pain management (spinal cord stimulators and intrathecal drug delivery systems). He also

serves as a Reviewer for several pain journals.



Yogesh B. Gianchandani (S'83–M'85–SM'04–F'10) received the B.S., M.S., and Ph.D. degrees in electrical engineering, with focus on microelectronics and microelectromechanical systems.

He is currently a Professor at the University of Michigan, Ann Arbor, with a primary appointment in the Department of Electrical Engineering and Computer Science and a courtesy appointment in the Department of Mechanical Engineering. He also serves as the Director of the Engineering Research Center for Wireless Integrated Microsystems. His

research interests include all aspects of design, fabrication, and packaging of micromachined sensors and actuators. He has published about 250 papers in journals and conference proceedings and is the holder of 30 U.S. patents issued or pending.

Dr. Gianchandani was a Chief Coeditor of *Comprehensive Microsystems: Fundamentals, Technology, and Applications*, published in 2008. He serves several journals as an Editor or a Member of the Editorial Board. He served as a General Cochair for the IEEE/ASME International Conference on Micro Electro Mechanical Systems in 2002. From 2007 to 2009, he also served as the National Science Foundation Program Director for Micro and Nano Systems within the Electrical, Communication, and Cyber Systems Division.